

Corrosion of steel bars in saturated $\text{Ca}(\text{OH})_2$ and concrete pore solution

Amir Poursaee^C

*School of Civil Engineering, Purdue University, West Lafayette
Indiana, 47907, USA*

Abstract

Testing steel in solution has the advantage of avoiding the long time necessary for chlorides to penetrate the concrete cover. It is well known that steel in high alkaline environments is passive and the protective capability of the passive film increases with pH. The pH of saturated calcium hydroxide solution is lower than concrete pore solution which does induce passivation but not to the degree encountered by steel in good quality concrete. Nevertheless, saturated calcium hydroxide has been used in many studies of rebar corrosion as a substitute for pore solution. This paper discusses the electrochemical behavior of low carbon steel bars in chloride free and chloride contaminated pore solution and saturated calcium hydroxide solution. Results show that the passive film on the steel immersed in pore solution and saturated $\text{Ca}(\text{OH})_2$ have similar composition. However, as a result of lower pH in saturated $\text{Ca}(\text{OH})_2$ solution, the passive layer formed in this solution is less protective and does not offer enough passivity to steel to simulate a realistic concrete environment.

Keywords: Pore solution; Corrosion; $\text{Ca}(\text{OH})_2$, Raman spectroscopy, Cyclic polarization, Linear Polarization Resistance

1. Introduction

The long time necessary for chlorides to penetrate the concrete cover can be avoided by testing the steel in concrete simulated pore solution, which is mainly consisted of saturated calcium hydroxide ($\text{Ca}(\text{OH})_2$), sodium hydroxide (NaOH) and potassium hydroxide (KOH) with the pH ~ 13.5 [1, 2]. However, in numerous studies of rebar corrosion, saturated $\text{Ca}(\text{OH})_2$ has been used as a substitute for pore solution [3-9]. The pH of saturated calcium hydroxide solution is about 12.6 [10]. The capability of the passive film to protect the steel against corrosion increases with pH [11]. Consequently, the passive layer induced by saturated calcium hydroxide does induce passivation but not to the degree encountered by steel in good quality concrete.

^C Corresponding Author: Amir Poursaee
Email: poursaee@purdue.edu

Moreover, the other ions present in pore solution, particularly, sodium and potassium, may also play a role in the passivation and corrosion processes.

However, the nature of the passive film due to using saturated Ca(OH)₂ and simulated pore solution was not compared together in the previous studies. The required time of passivation of steel in concrete was determined for steel in pore solution [12] but not in saturated calcium hydroxide. In this paper, the time required for steel reinforcing bar to be passivated in synthetic pore solution compared to that for saturated calcium hydroxide solution. Potentiostatic linear polarization resistance (LPR) and half-cell potential techniques were used to determine the time required for passivation. The surface condition of the steel bars, after immersion in concrete pore solution and saturated calcium hydroxide, was studied by Raman spectroscopy. In addition, chloride induced corrosion behavior of the steel bars immersed in chloride contaminated synthetic pore solution and saturated Ca(OH)₂ was studied, using cyclic polarization technique. Raman spectroscopy and microscopic analysis were used to study the corrosion products and surface condition of the steel bars after corrosion, respectively.

2. Materials and methods

Two sets of samples have been made for this experiment: steel bars in simulated concrete pore solution (Type I cement), with the composition shown in Table 1, and in saturated Ca(OH)₂.

TABLE 1. CHEMICAL COMPOSITION OF THE SYNTHETIC PORE SOLUTION

Compound	mol/liter
NaOH	0.1
KOH	0.3
Ca(OH) ₂	0.03
CaSO ₄ .H ₂ O	0.002

It should be mentioned that the pore solution composition shown in Table 1 is based on the pore solution extraction from cement paste samples with w/c=0.42 which were wet cured for 7 days. For each solution, two containers with three low carbon steel bars [13] with smooth surface and diameter of 5 mm were prepared as illustrated in Figures 1.

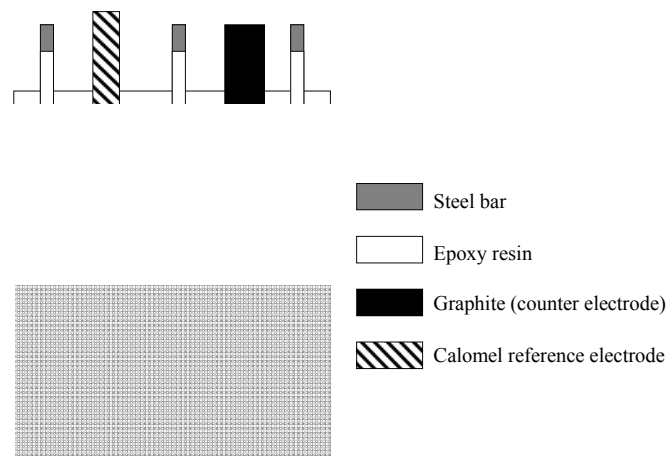


Figure 1. Schematic view of the setup used for the experiment

Surface of each bar was ground using 600 grit sand paper and decreased in acetone. To prevent extraneous effects, the both ends of the bars were coated with epoxy resin to define the exposed length (30 mm of the bar). After installing the required components, all containers were sealed to avoid carbonation. All samples were connected to automatic data acquisition system [14] and the corrosion current density, by using potentiostatic LPR, and half-cell potential of each steel bar were measured every hour for 7 days. Saturated calomel electrode and graphite rod were used as a reference electrode and counter electrodes, respectively. LPR measurements were performed by applying a potential in the range of ± 10 mV about the half-cell potential. After one week exposure of steel to each solution, 10 wt% chloride (as sodium chloride) was added to one of the containers of each solution to simulate the severe corrosion condition. 24 hours after adding salt, the corrosion activity of the bars in the chloride contaminated containers was investigated using cyclic polarization resistance. The scan was started at -200 mV below the half-cell potential, increased to +200 mV and decreased to -200 mV versus the half-cell potential, with the scan rate of 0.1 mV/s. The steel bars were kept in the chloride free container of each solution for two months and the surface condition of the steel bars was studied with Raman spectroscopy technique. The solution of each container was refreshed every week during this period of time.

3. Results and discussion

The corrosion current densities and half-cell potential values measured over a period of 168 hours (7 days) are shown in Figure 2.

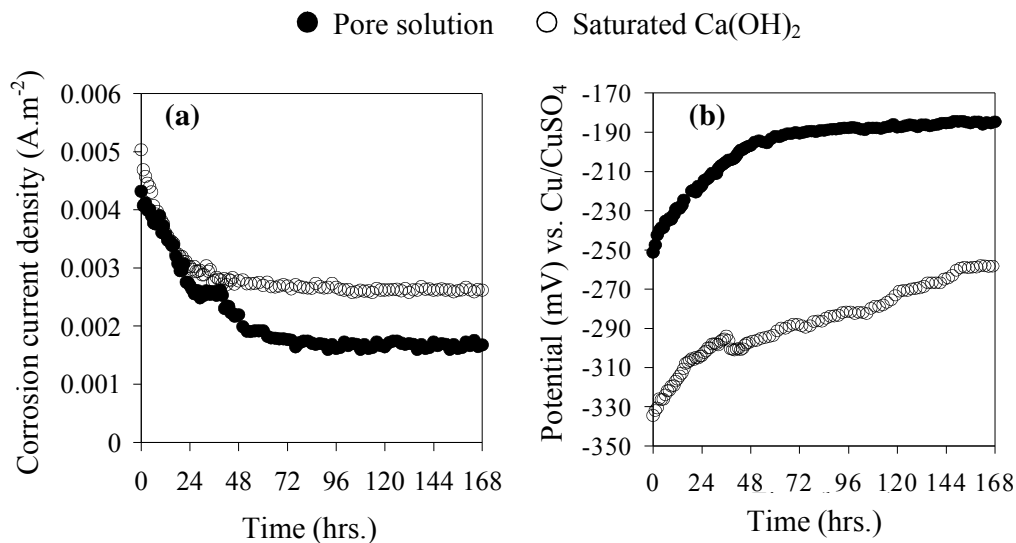


Figure 2. (a) Corrosion current density and (b) half-cell potential values of the steel bar immersed in synthetic pore solution and saturated $\text{Ca}(\text{OH})_2$ for a week.

The results show that the corrosion current density for simulated pore solutions drops to about 1×10^{-3} A.m^{-2} which is the expected value for passive state (10^{-3} to 10^{-4} A.m^{-2}) [7]. However, this value for saturated $\text{Ca}(\text{OH})_2$ solution is about 3×10^{-3} A.m^{-2} . In both solutions, the current density was stabilized after about 48 hours.

The half-cell potential values of the specimens immersed in simulated pore solution stabilized at about 48 hours. However, the potential of the bars in saturated $\text{Ca}(\text{OH})_2$ started stabilizing after about 144 hours. The potential of all specimens in pore solution were more

positive than -200 mV, which is the “90% probability of no corrosion” range while the potential of the specimens immersed in saturated Ca(OH)₂ were between -350 and -200 mV, which is the “uncertainty” range based on ASTM C876 criteria for corrosion [13]. It should be noted that for comparison purpose, with the ASTM G 876, all the measured potentials versus calomel reference electrode were converted to Cu/CuSO₄.

Results of Raman spectroscopy are shown in Figures 3 and the main Raman bands of reference iron oxide compounds are given in Table 2 [15-18]. As can be seen, the passive layer in both solutions has the same composition. However, the steel bar immersed in simulated concrete pore solution shows higher intensity of the Raman peaks compare to that immersed in saturated Ca(OH)₂ which is the indication of forming more thicker and more protective passive layer on the surface of the steel bar in pore solution.

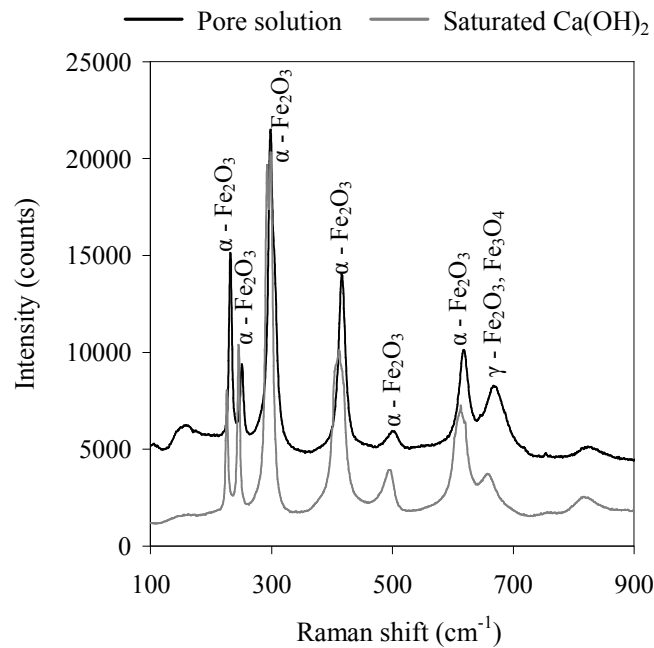


Figure 3. Raman spectra of steel immersed in pore solution and saturated Ca(OH)₂ for 2 months

TABLE 2. MAIN BANDS OF REFERENCE IRON OXIDE COMPOUNDS (IN cm⁻¹)

Magnetite	Hematite	Maghemite
Fe ₃ O ₄	α-Fe ₂ O ₃	γ-Fe ₂ O ₃
289	225	265
319	247	300
418	295	350
550	412	395
670	500	505
	613	660

Results from the electrochemical measurements and Raman spectroscopy in chloride free solutions imply that when the steel exposes to saturated Ca(OH)₂ solution, the passive film start to form but it is less protective than the film forms when the steel is exposed to pore solution. This different is attributed to the higher pH of the synthetic pore solution compare to the pH in

the saturated calcium hydroxide solution. While the composition of the passive film is independent from the pH of the alkaline solution, the thickness of the passive film increases by increasing the pH [19].

One week after exposure of the steel bars to the chloride free solutions, 10 wt% chloride (as NaCl) was added to each solution to simulate severe corrosion condition. Corrosion activity of the bars in both chloride contaminated pore solution and saturated $\text{Ca}(\text{OH})_2$ solution was investigated using cyclic polarization method. Figure 4, shows the cyclic curves for one of the steel bars in each solution. It should be mentioned that the test was performed on all three bars in each solution and the results were very similar.

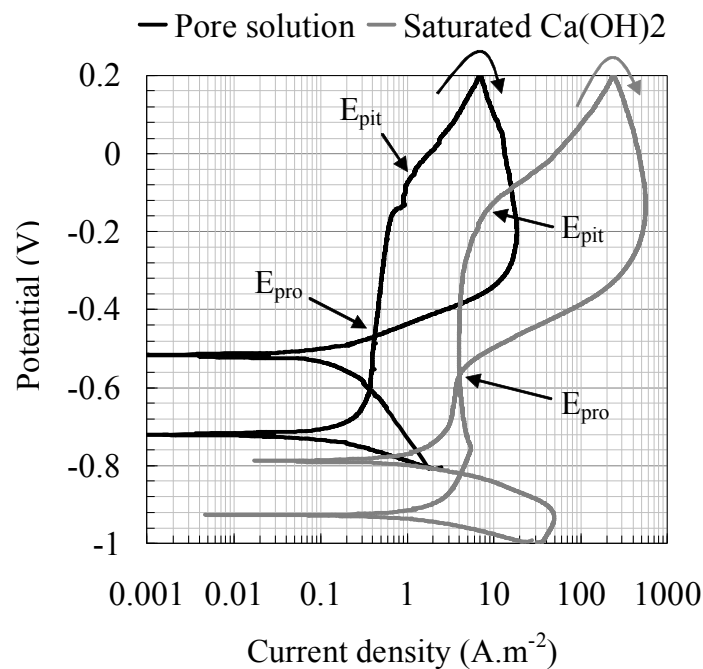


Figure 4. Cyclic polarization curves of steel bars exposed to chloride contaminated pore solution and saturated calcium hydroxide

As can be seen, in both solutions, the pitting potential (E_{pit}) is more positive than the protection potential (E_{pro}) which is an indication of pitting corrosion. In addition, the direction of the curves on the peak potential in both cases show active and pitting corrosion behaviors. However, steel in chloride contaminated pore solution shows more positive half-cell potential and lower corrosion rate compared to those for steel in contaminated $\text{Ca}(\text{OH})_2$. The corrosion current density of steel in $\text{Ca}(\text{OH})_2$ solution is about 5 times higher than that in pore solution. The size of the cyclic polarization loop for contaminated saturated $\text{Ca}(\text{OH})_2$ is also larger than that for pore solution which illustrates greater tendency to pit in $\text{Ca}(\text{OH})_2$ solution than pore solution.

An algorithm was developed using ImageJ [20], which is an open source Java-based software program developed at the National Institutes of Health, in order to estimate the corroded surface area. After taking pictures from the surface, a threshold was applied to the image to separate the dark and light portions (i.e., the corroded and non-corroded surface areas). This process is shown in Figure 5 for one of the steel bars in pore solution and saturated $\text{Ca}(\text{OH})_2$ solution. Results show that about 60% of the surface area of the steel immersed in chloride contaminated $\text{Ca}(\text{OH})_2$ is corroded while this number is about 30% for steel in pore solution

containing chloride. These numbers were used to calculate the corrosion current density in Figure 4.

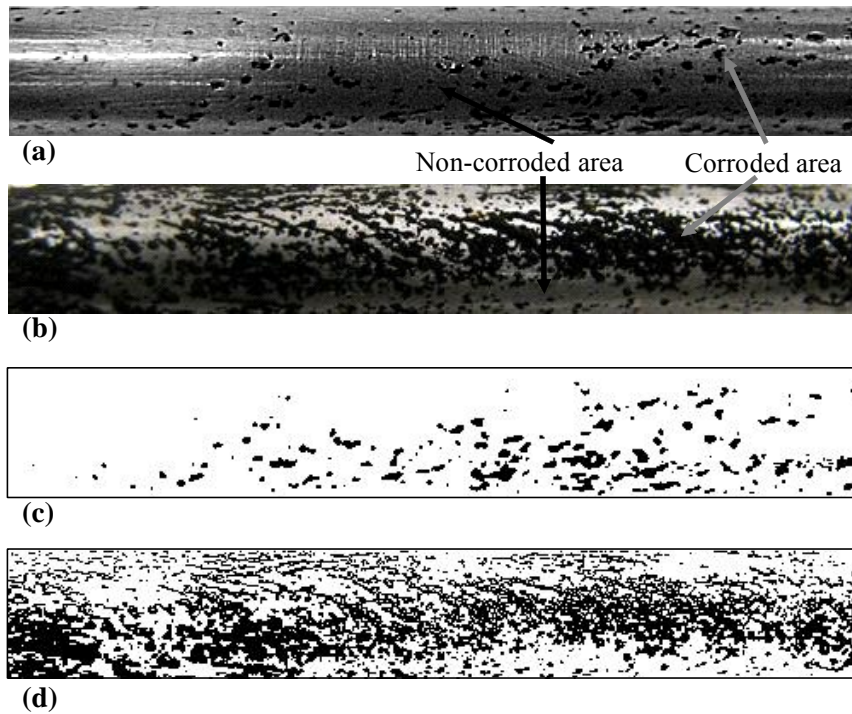


Figure 5. Surface of the steel bars after the cyclic polarization test in (a) pore solution, (b) saturated $\text{Ca}(\text{OH})_2$. The results of image analyzed of (a) is shown in (c), the results of image analyzed of (b) is shown in (d)

After the test, corrosion products were removed using inhibited acid solution [21] and the morphology of corrosion attack (pits) was observed. As shown in Figure 6, pits formed due to chloride attack in saturated $\text{Ca}(\text{OH})_2$, are deeper and larger compare to those in pore solution.

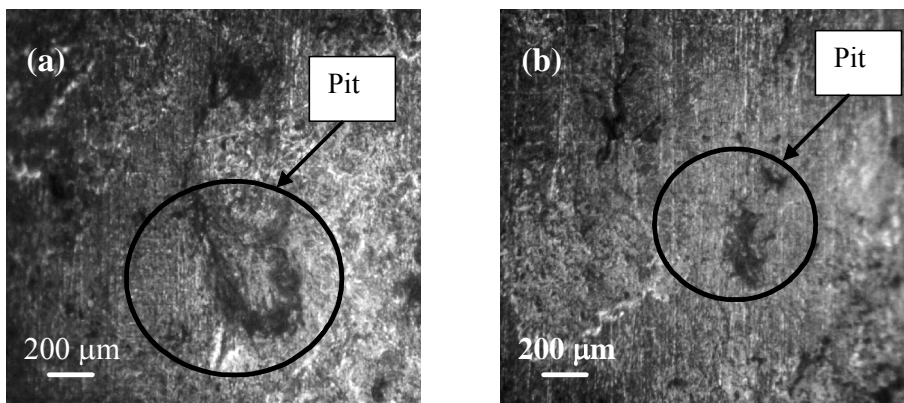


Figure 6. Microscopy images of metal surface after cyclic polarization test in chloride contaminated (a) saturated $\text{Ca}(\text{OH})_2$ and (b) simulated pore solution

From cyclic polarization test and also the visual and microscopic observation it is obvious that steel bars in chloride contaminated saturated $\text{Ca}(\text{OH})_2$ solution corrode more severe than

those immersed in chloride contaminated pore solution. It seems that more severe corrosion in chloride contaminated $\text{Ca}(\text{OH})_2$ solution is mainly due to the formation of the less protective passive layer on the steel bars immersed in saturated $\text{Ca}(\text{OH})_2$ before adding the chloride to the system.

Corrosion products on the surface of steel bars in both chloride contaminated solutions were also analyzed, using Raman spectroscopy. Figure 7 shows a typical Raman shift obtained from the corrosion products. No significant different was observed between the corrosion products formed in two solutions. The corrosion products are consisted of hematite ($\alpha\text{-Fe}_2\text{O}_3$), magnetite (Fe_3O_4) and maghemite ($\gamma\text{-Fe}_2\text{O}_3$).

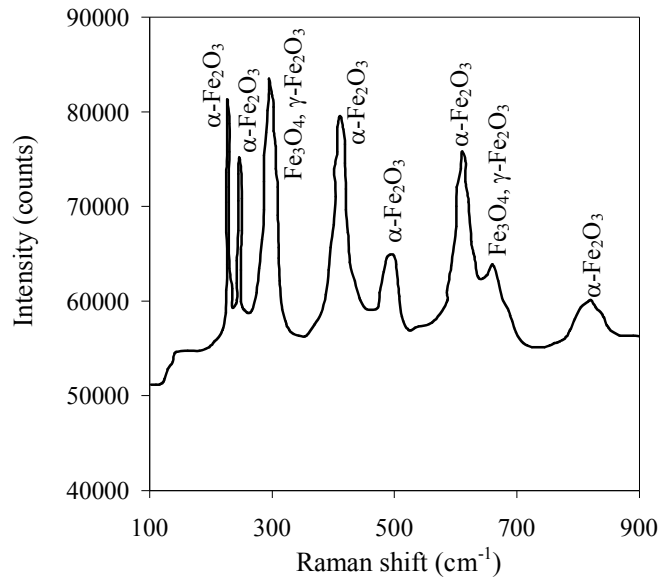


Figure 7. Typical Raman spectra of the corrosion products on the steel bars in chloride contaminated pore solution and saturated $\text{Ca}(\text{OH})_2$

4. Summary and Conclusions

- The passive film on the steel in pore solution and saturated $\text{Ca}(\text{OH})_2$ developed relatively at the same time and have similar composition. However, as a result of lower pH in saturated $\text{Ca}(\text{OH})_2$ solution, the passive layer formed in this solution is less protective and does not offer enough passivity to steel to simulate a realistic concrete environment.
- Chloride induced corrosion is more severe for the steel exposed to chloride contaminated saturated $\text{Ca}(\text{OH})_2$ solution compare to that exposed to chloride contaminated pore solution. The weaker passive film on the surface of steel, formed in saturated $\text{Ca}(\text{OH})_2$ compared to that forms in pore solution, is the main reason of such behavior.
- The corrosion product due to chloride induced corrosion in both pore solution and $\text{Ca}(\text{OH})_2$ are similar and have the same compositions.
- Therefore, if solutions, are to be used as the test environment, these should, to the greatest degree, mimic the pore solution of the specific concrete in question and using saturated $\text{Ca}(\text{OH})_2$ is not sufficient and it does not provide enough passivity to steel bar to simulate the actual concrete environment.

References

- [1] Andrade C., Merino P., Novoa X. R., Perez M. C., Solar L. *Passivation of reinforcing steel in concrete*. Materials Science Forum 1995;192-194:861.
- [2] Hansson C. M. *Comments on electrochemical measurements of the rate of corrosion of steel in concrete*. Cement and Concrete Research 1984;14:574.
- [3] Ramirez E., Gonzalez J. A., Bautista A. *The protective efficiency of galvanizing against corrosion of steel in mortar and in Ca(OH)₂ saturated solutions containing chlorides*. Cement and Concrete Research 1996;26:1525.
- [4] Hou J., Chung D. D. L. *Effect of admixtures in concrete on the corrosion resistance of steel reinforced concrete*. Corrosion Science 2000;42:1489.
- [5] Gonzalez J. A., Miranda J. M., Otero E., Feliu S. *Effect of electrochemically reactive rust layers on the corrosion of steel in a Ca(OH)₂ solution*. Corrosion Science 2007;49:436.
- [6] Nakayama N. *Inhibitory effects of nitrilotris (methylenephosphonic acid) on cathodic reactions of steels in saturated Ca(OH)₂ solutions*. Corrosion Science 2000;42:1897.
- [7] Nakayama N., Obuchi A. *Inhibitory effects of 5-aminouracil on cathodic reactions of steels in saturated Ca(OH)₂ solutions*. Corrosion Science 2003;45:2075.
- [8] Gonzalez J. A., Cobo A., Gonzalez M. N., Otero E. *On the effectiveness of realkalisation as a rehabilitation method for corroded reinforced concrete structures*. Materials and Corrosion 2000;51:97.
- [9] G. Blanco, A. Bautista, H. Takenouti. *EIS study of passivation of austenitic and duplex stainless steels reinforcements in simulated pore solutions*. Cement & Concrete Composites 2006;28:212.
- [10] Lide D. R. *CRC Handbook of chemistry and physics*. New York, NY: CRC Press, 1999.
- [11] Verink E. D., Pourbaix M. *Pitting potentials versus pH*. Corrosion 1971;27:495.
- [12] Poursae A., Hansson C. M. *Reinforcing steel passivation in mortar and pore solution*. Cement and Concrete Research 2007;37:1127.
- [13] ASTM. *C876-09: Standard Test Method for Half-cell Potentials of Uncoated Reinforcing Steel in Concrete*. vol. 03.02. 2009. p.446.
- [14] Poursae A. *Automatic system for monitoring corrosion of steel in concrete*. Advances in Engineering Software 2009;40:1179–1182.
- [15] Dunn D. S., Bogart M. B., Brossiaand C. S., Cragnolino G. A. *Corrosion of iron under alternate wet and dry conditions*. Corrosion 2000;56:470.
- [16] Balasubramaniam R., Kumar A. V. R., Dillmann P. *Characterization of rust on ancient Indian iron*. Current Science 2003;58:1546.
- [17] Dunnwald J., Otto A. *An investigation of phase transitions in rust layers using Raman spectroscopy*. Corrosion Science 1989;29:1167.
- [18] Oh S. J., Cook D. C., Townsend H. E. *Characterization of iron oxides commonly formed as corrosion products on steel*. Hyperfine Interactions 1998;112:59.
- [19] Miserque F., Huet B., Azou G., Bendjaballah D., L'Hostis V. *X-ray photoelectron spectroscopy and electrochemical studies of mild steel FeE500 passivation in concrete simulated water*. Journal de Physique IV 2006;136:89.
- [20] *ImageJ*. National Institutes of Health, <http://rsbweb.nih.gov/ij/>.
- [21] ASTM. *G1-90: Standard Practice for Preparing, Cleaning, and Evaluating Corrosion Test Specimens*. ASTM, 1999.